Supplementary information

The biosynthetic pathway for aurofusarin in *Fusarium graminearum* reveals a close link between the naphthoquinones and naphthopyrones.

Rasmus J.N. Frandsen (1); Nikoline J. Nielsen (2); Nicolai Maolanon (2); Jens C. Sørensen (2) ; Stefan Olsson (1); John Nielsen (2), and Henriette Giese (2).

Department of Ecology (1) and Department of Natural Sciences (2), The Royal Veterinary and Agricultural, University, DK-1871 Frederiksberg C, Copenhagen, Denmark

* Corresponding author; Rasmus J.N. Frandsen, Tel. +45 35282608, Fax. +45 35282606,
E-mail raf@kvl.dk

Page 1 to 5 Chemical characterization and identification of intermediates
Page 6-7 Table S1 – The primers used in the experiment.

Materials and Methods

Samples for HPLC-UV-MS and NMR analysis were prepared with an ASE 200 accelerated solvent extractor equipped with a solvent controller, both from Dionex, operated at elevated pressures and temperatures, thus increasing the efficiency of the extraction procedure. The extraction procedure is highly reproducible and the extracts were subjected to LC-PDA-MS analysis without further sample preparation. Preliminary extraction was performed on approximately 1 g of biological material packed with Spe-ed Matrix (Applied Separations, USA) in a 33 ml extraction cell. The samples was extracted with a) >99 % heptane (Riedel-deHaën (Germany)), b) >99.5 % ethyl acetate (Fluka (Germany)), c) >99.9 % methanol (Sigma-Aldrich (Germany)), and d) 70% methanol for separation of extracted compounds by solvent polarity. The extracts were evaluated by LC-PDA-MS with respect to purity and amount of the desired analyte. The bulk extraction was performed on more densely packed extraction cells by de-fatting with heptane followed by continuous extraction with the previously chosen solvent until extraction recovery approaches unity. Nor-rubrofusarin and rubrofusarin were extracted from agar with ethyl acetate, which gave extracts of high purity facilitating the following work-up. ASE parameterization was as follows: preheat 0 min; heat 5 min; static 5 min; flush volume 50%; purge 120 s; cycles 2; pressure 2000 psi; temperature 40°C.

LC-PDA-MS fingerprinting of extract:

The extracts and further work-ups were characterized by LC-PDA-MS. The system consisted op a Waters 2795 separation module with degasser, temperature regulated autosampler and a column oven hyphenated with a Waters 996 photodiode array (PDA) detector and a Micromass LCT high-resolution time of flight mass spectrometer, all equipment supplied by Waters. Ionisation was performed in positive electrospray mode. MS parameterization were as follows: Pirani pressure 1.0e(-1) mbar, Penning pressure 2.3e(-7) mbar, nebulizer gas (N2) flow 95 L/hr, desolvation gas flow 5600 L/hr, capillary voltage 2.9 kV, sample cone voltage 30 V, RF lens 300 V, extraction cone voltage 3 V, desolvation temperature 350°C and source temperature 120°C. PDA-detection was done in the 210-400 nm window. Separation was achieved on one of two LC columns: a) Sunfire C18 (dimensions 2.1 x 50 mm, particle size 3.5 um) or b) Xterra Phenyl (dimensions 2.1 x 100 mm, particle size 3.5 um) both from Waters, with a linear gradient from 100% A: 0.1% formic acid in 5:95 (v/v) acetonitrile:water to 100% B: 0.1% formic acid in 5:95 (v/v) water:acetonitrile in 25 or 55 minutes followed by 1 minute of 100% B and 4 minutes of 100% A (formic acid (88-91%) from Fluka (Switzerland) and acetonitrile (>99.5 %) from Sigma-Aldrich (Germany)). Generally the naphthoquinones and –pyrones showed the best separation on the C18 column. All preliminary extracts were analyzed with wild type extracts for verification of metabolite novelty. Relevant extracts were combined and evaporated to dryness on a rotary evaporator R-200 equipped with heating bath B-490 and vacuum controller V-800, all from Büchi. MassLynx software 4.0 was used for data processing.

Preparative LC with PDA detection:

The crude extract was redissolved in a mobile phase compatible solvent, most often methanol. Particles were precipitated by centrifugation on an Eppendorf centrifuge at 11000 x g for 1 minute. The supernatant was used for analytical LC and preparative LC collection of the target analyte, while the precipitate was re-extracted with mobile phase compatible solvent. The procedure was repeated until insignificant amounts of the target analyte were extracted from the precipitate. The LC-system consisted of a Waters 2525 binary gradient module equipped with a column fluidic organizer, an UV fraction manager and a Waters 2767 sample manager for fully automated fraction collection coupled with a Waters 2996 PDA detector. PDA-detection was carried out in the 215-400 nm window. The analytical column was a Xterra C18 MS (dimensions 4.6 x 100 mm, particle size 5 um) and the preparative column a Xterra C18 Prep MS (dimensions 19 x 100 mm, particle size 5 um) both from Waters. Mobile phases consisted of A: water with or without 0.1% TFA and B: acetonitrile with or without 0.1% TFA. Short water:acetonitrile gradients with acceptable analyte resolution were established using the analytical system. Trifluoroacetic acid (>98%) from Riedel-deHaën (Germany) was added to the mobile phase. This method can then be scaled to preparative LC by just copying the gradient and increasing the flow rate. MassLynx software with FractionLynx version 4.0 was used for data processing.

NMR

Spectra were recorded in $CDCl_3$ on a Bruker 300 MHz NMR spectrometer. A drop of DMSO was added to increase solubility in some cases. 1D spectra were processed using MestReC 4.7.4 freeware. 2D spectra were auto processed with using XWIN-NMR version 3.5.

High-resolution MS

The accurate mass determinations were performed on the previously describes TOF mass spectrometer with a more than 10 ppm accuracy using leucine enkephalin (96 % from Sigma (Germany)) or on occasions a PEG 200-1000 (polyethylene glycols from Sigma (MO, USA)) solution as internal standard to correct for m/z drift.

Results

The Δ*aurJ* mutant produces nor-rubrofusarin (Fig. S1).

The UV-spectrum (Fig. S2) was recorded in MeCN:water and had λ_{max} at 278, 224, 253, 410, 328 nm. The mass was determined by ESI-TOF-MS to 259.0612 $[M+H]^+$ (calc. exact mass 259.0606). The ^1H NMR spectrum was ($CDCl_3$ with a drop of DMSO added, 300 MHz) δ 2.24 (3H, s, Me), δ 5.85 (1H, s, H-3), δ 6.29 (1H, d, J=2.14, H-7), δ 6.45 (1H, d, J=2.17, H-9), δ 6.73 (1H, s, H-10), δ 9.5 (1H, s, OH-6), δ 15.9 (1H, s, OH-5) and the ^{13}C NMR spectrum δ 20.6 (Me), δ 100.0 (C-10), δ 100.8 (2C, C-7, C-9), δ 101.8 (C-12), δ 105.5 (C-13), δ 105.8 (C-3), δ 140.1 (C-14), δ 151.9 (C-11), δ 158.6 (C-6), δ 160.9 (C-8), δ 161.9 (C-5), δ 168.5 (C-2), δ 183.6 (C-4). Compared to the ^1H and ^{13}C chemical shifts reported by Lee *et al.* (1998), the chemical shifts in DSMO are similar, while those recorded $CDCl_3$ correlate within 1.2 ppm. No OH-5 proton shift was observed in $CDCl_3$. One bond ^1H-^{13}C correlations were confirmed by HSQC, and two of three possible four bonds ^1H-^1H correlations were confirmed by COSY. Yield from freeze-dried agar was 0.03% (dw).

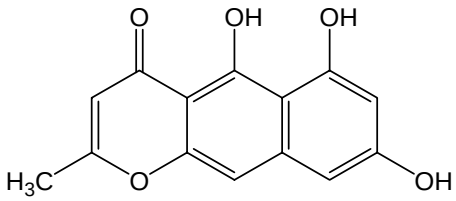

Fig. S1 Structure of nor-rubrofusarin.

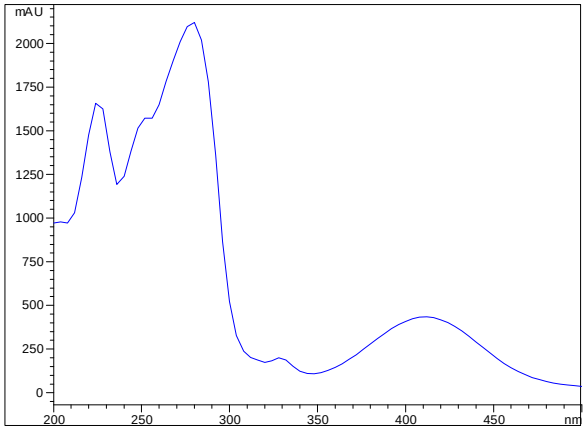

Fig. S2 UV-spectrum of nor-rubrofusarin.

The Δ*gip1* and the Δ*fmo* mutants produce rubrofusarin (Fig. S3).

The UV spectrum (Fig. S4) was recorded in MeCN:water and had λ_{max} at 277, 224, 253, 404, 325 nm. The mass was determined to ESI-TOF-MS 273.0760 $[M+H]^+$ (calc. exact mass 273.0763). The ^1H NMR spectrum in $CDCl_3$ (300 MHz) was δ 2.40 (3H, s, Me), δ 3.90 (3H, s, OMe), δ 6.02 (1H, s, H-3), δ 6.48 (1H, d, J=2.21 Hz, H-7), δ 6.59 (1H, d, J=2.21 Hz, H-9), δ 6.98 (1H, s, H-10), δ 9.67 (1H, s, OH-6), δ 15.94 (1H, s, OH-5); ^{13}C NMR ($CDCl_3$, 75 MHz) δ 21.0, δ 55.4, δ 98.0, δ 100.6, δ 101.2, δ 102.9, δ 106.5 (2C), δ 140.2, δ 152.5, δ 158.7, δ 162.0, δ 162.9, δ 168.8, δ 184.1. All proton chemical shifts correlated within 0.07 ppm and ^{13}C chemical shifts within 0.1 ppm of those published by Alemayehu *et al.* (1993). Here the H-10 proton shift appeared at 6.98 ppm, which is a 0.3 ppm deviation from that of Alemayehu *et al.* (1993) which reported it at 6.69 ppm. The lack of accordance could be due to a typing mistake. COSY-, HSQC-, HMBC-, TOCSY- and NOESY-spectra confirmed the identity of rubrofusarin.

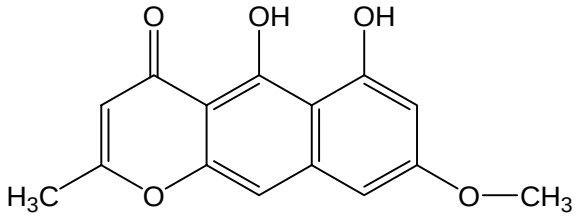

Fig. S3 Structure of rubrofusarin.

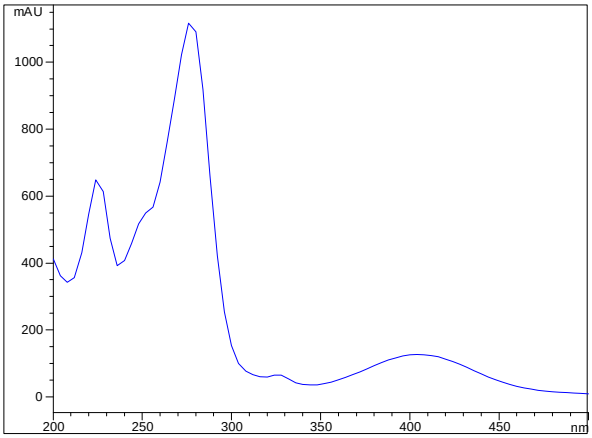

Fig. S4 UV-spectrum of rubrofusarin.

No other up-regulated metabolites were identified in the mutants.

Discussion and conclusion

During the structural determination, we saw dimerization of $C_{15}H_{12}O_5$-compounds e.g. dimerization of rubrofusarin; dimerization of $C_{15}H_{10}O_6$-compounds e.g. formation of aurofusarin from oxidized rubrofusarin, coupling of $C_{15}H_{12}O_5$- and $C_{15}H_{10}O_6$-compounds e.g. formation of fuscofusarin from rubrofusarin and oxidized rubrofusarin, as well as spontaneous oxidation of rubrofusarin i.e. $C_{15}H_{12}O_5$ to $C_{15}H_{10}O_6$, which could represent the aurofusarin monomer. At room temperature the oxidation of rubrofusarin proceeds rapidly, and dimers of oxidation products was always more abundant than heteromers. Dimers of rubrofusarin were only observed when stored primarily under argon. Thus, we expect oxidation to occur prior to dimerization under *in vitro* conditions. The observation of a $C_{30}H_{20}O_{12}$-compound suggests the presence of a dimeric product with two more hydrogens than aurofusarin.

Introduction of a C-9 hydroxyl group in rubrofusarin and further oxidation of the formed hydroquinone to quinone could possibly proceed by an UV- or VIS-initiated radical reaction in the presence of iron species, water and oxygen, all of which could be present in our NMR tube with isolated rubrofusarin. Examples of radical initiation and scavenging as well as radical induced oxidation in such systems are given in Rivas *et al*. (2005), Tryba *et al*. (2005) and Zazo *et al*. (2005) (Fig. S5).

Quinones and pyrones have been oxidatively coupled at carbonyl α-carbons by the transition metal palladium (Itahara, 1985). It is likely that a transition metal containing enzyme, such as the Cu-containing laccases, could catalyze this reaction *in vivo*. Quinones with electron donating substituents e.g. methoxy functionalities are known to have an enolate resonance-form (Norman and Coxon, 1993). Another hypothesis is that the oxidative coupling proceeds

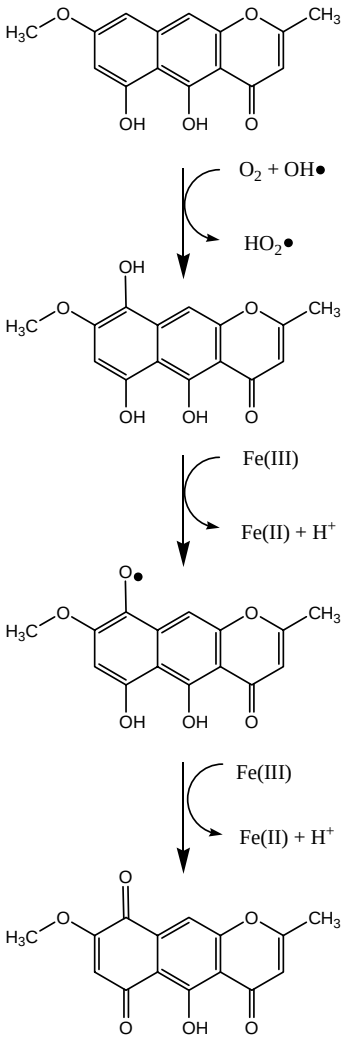

Fig. S5 *In vitro* radical initiated oxidation of rubrofusarin resulting in formation of hydroquinone and quinone forms of rubrofusarin. The transformation is dependent on molecular oxygen and is driven the reduction of FeIII to FeII.

by Michael-attack from this resonance-form onto another quinone molecule to yield an unaromatized zwitterionic reaction intermediate containing two more hydrogens than aurofusarin. Subsequently, the unaromatized dimer could loose two hydrogens and thereby regain aromaticity (Fig. S6).

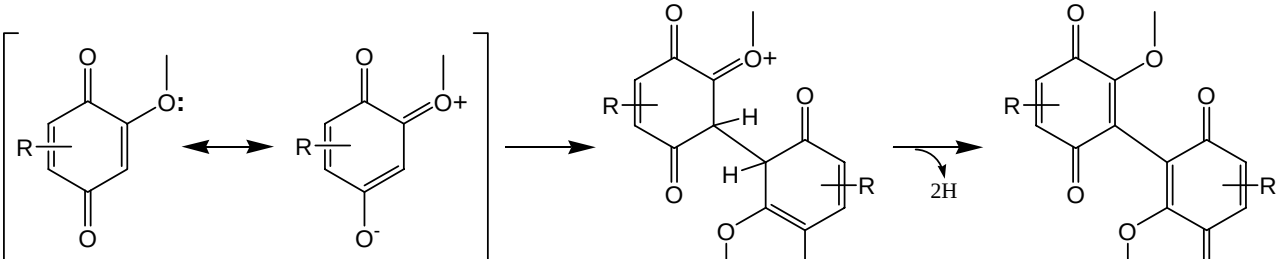

Fig. S6 Possible reaction mechanism for dimerization of quinones under *in vitro* conditions. Oxidative coupling by methoxy-induced Michael attack between keto/enol forms of quinone.

It is not clear how the final loss of two hydrogens can proceed uncatalyzed, but the gain of aromaticity could be the driving force for the *in vitro* reaction. The suggested methoxy-initiated oxidative coupling would explain the reactivity of rubrofusarin compared to nor-rubrofusarin, as it would explain the presence of a compound of mass 573 (presumably unaromatized aurofusarin with two more hydrogens) that elute close to aurofusarin in the wild type extracts. Oxidation could proceed via a light-induced iron-catalyzed radical reaction if water and oxygen is present. The oxidative coupling could be metal-catalyzed, possibly initiated by methoxy-induced Michael attack. Intermediates and resonance structures with separation of charge are assumed to be stabilized by protonation.

References

Alemayehu, G., Abegaz, B., Snatzke, G., and Duddeck, H. (1993) Bianthrones from Senna longiracemosa. Phytochemistry 32(5): 1273-1277.

Itahara, T. (1985) Oxidative coupling of quinones and aromatic compounds by palladium(II) acetate. J. Org. Chem. 50: 5546-5550.

Lee, H.J., Park, J.C. and Choi, J.S. (1998) The ^{13}C-NMR Assignment of Nor-rubrofusarin having Strong Radical Scavenging Effect on 1,1-Diphenyl-2-picrylhydrazyl Radical. *Natural Product Sciences* 4(2): 95-99.

Rivas, F.J., Frades, J., Alonso, M.A., Montoya, C., and Monteagudo, J.M. (2005) Fenton's oxidation of food processing wastewater components. Kinetic modeling of protocatechuic acid degradation. J. Agric. Food Chem., 53(26): 10097-10104.

Tryba, B., Toyoda, M., Morawski, A.W., Inagaki, M. (2005) Modification of carbon-coated TiO2 by iron to increase adsorptivity and photoactivity for phenol. Chemosphere 60: 477-484.

Zazo, J.A., Casas, J.A., Mohedano, A.F., Gilarranz, M.A., Rodríguez, J.J. (2005) Chemical pathway and kinetics of phenol oxidation by Fenton's reagent. Environ. Sci. Technol. 39: 9295-9302.

Table S1 Primers for targeted gene replacement and verification of replacement events. Restriction sites are highlighted. # Product length with the Hyg1 primer and ¤ product length with Hyg2 primer. * These primers were used for Xi-cloning (*in vivo* homolog recombination).

Primer name	Sequence (5' to 3')	Length (bp)	Restriction site	Product length
aurR1-A1	**CGTCGACC**ACCCGCGAAGCCATTTGAGG	28	*Sal*I	1,963 bp
aurR1-A2	**CACTAGT**TTGCCGCAGCGAACTTTTGACTTG	31	*Spe*I	
aurR1-A3	**CGGGCCC**CAGCCCCGTATCAACCAAAACTCC	31	*Xma*I	1,987 bp
aurR1-A4	**CCCGGG**GTAAGCGGCACTCCCAACACTCGT	30	*Apa*I	
aurR1-T1	AGCCCGGCGTGATTTCTTG	19	-	3,838 bp #
aurR1-T2	TGGAGATACTGATGTGCCGAGATG	24	-	2,760 bp ¤
aurR1-T3 (CDS)	TTCCACAGACCCCCTTCTCCGCA	23	-	1,187 bp
aurR1-T4 (CDS)	TGACCTCGAGCTTCTTTCGTACATCCAGG	29	-	
aurO-A1H *	**CCAGTGAATTCGAGCTCGGTACCAAGGCCC**-CCGCTCGGTGTCCTTTCCATCATTA	55	-	2,127 bp
aurO -A2H *	**CTTGCGCGCCTAGGCGGCCGTGGCCAGCCC**-AGCCCCCTTTCCTCCCGTCCCTACT	55	-	
aurO -A3	**ACTAGT**CCGCTTGGTTGATGGTGTGGA	27	*Spe*I	2,148 bp
aurO -A4	**AAGCTT**AGGCTCTGCGGGCATCTACTCTGGCTCTA	35	*Hind*III	
aurO -T1 (CDS)	AGCCCAGGATGCCCAGGTTCAC	22	-	823 bp
aurO -T2 (CDS)	AGGTCCAATCGTCTCGGCTTCAGG	24	-	
aurO -T3	TTACAAGCTGCCGCGAGAACATACGA	26	-	3,676 bp #
aurO -T4	CAGCTTCTTTGGGGGCGCATTTTTAC	26	-	2,286 bp ¤
aurR2-A1	**AAGCTT**CCGCGACGAGTCCTCAACACAGT	29	*Hind*III	1,912 bp
aurR2-A2	**CACTAGT**GGCCAGGGCATCGTCACAACAG	29	*Spe*I	
aurR2-A3	**CGGGCCC**CGCATAAGCCACGCATCAGTAAGC	31	*Xma*I	1,869 bp
aurR2-A4	**CCCGGG**CCGAGGGACTGGGCAAAGAACAT	29	*Apa*I	
aurR2-T1	AGACGGCTTGGGCAACACAGACGAGAACT	29	-	3,312 bp #
aurR2-T2	TACATTTTGGACAACTACCGCACCGACTTA	30	-	2,815 bp ¤
aurR2-T3 (CDS)	CTACACGGCCCGACAGTTCAGA	22	-	735 bp
aurR2-T4 (CDS)	AATTTTGCTTTGCCCGTAGTCG	22	-	
aurJ-A1	**CGTCGAC**GCTTGTCTCGACTGTGTTTT	27	*Sal*I	1,998 bp
aurJ-A2	**CACTAGT**CTTTGGTGGCTAGCTTTTCATA	29	*Spe*I	
aurJ-A3	**CGGGCCCC**GGTACCGATATCACTTCAG	27	*Xma*I	2,072 bp
aurJ-A4	**CCCGGG**ACCTCGTCTACATCATCCA	25	*Apa*I	
aurJ-T1	AAGATCCCAGAATTCACCCAAGTCAGC	27	-	3,560 bp #
aurJ-T2	CCTCAGCGTTCAATCCAAATATCAAAGTAA	30	-	2,896 bp ¤
aurJ-T3 (CDS)	GCGCGTCGAAGCATAAGATAGTTGTGTAA	29	-	983 bp
aurJ-T4 (CDS)	CAGAAAAGTGGCCAGGAAGTGTAAAGAAGA	30	-	
aurF-A1	**CCCGGG**AACACCTGGCGCATAGTCAAGTCT	30	*Xma*I	1,570 bp
aurF-A2	**GGGCCC**AGTGTTCGGGCTCGGGGATTA	27	*Apa*I	

aurF-A3	**ACTAGT**GAGGGTCACTGGTCATAGGAA	27	*Spe*I	2,016 bp
aurF-A4	**TTAATTA**AATTAGCAAAGAACAAGCCGACATC	32	*Pac*I	
aurF-T1 (CDS)	GGTCGTCTTCGCAATGGGAGCAG	23	-	527 bp
aurF-T2 (CDS)	GGTTTGTGATTGATGGGGCAGGAT	24	-	
aurF-T3	GCGCGTCGAAGCATAAGATAGTTG	24	-	2,984 bp #
aurF-T4	GATGGGCACACCTTGGTCAGATGG	24	-	2,406 bp ¤
gip1-A1	**GAGCTC**TGGCGCAAGATACGACGAAAAGAA	30	*Sac*I	1,877 bp
gip1-A2	**CCTAGG**CTAGTGGTGGCCCGAAGAAGGATT	30	*Avr*II	
gip1-A3	**ACTAGT**TTGCGTCGATGTCGGCTTGTTCTT	30	*Spe*I	1,561 bp
gip1-A4	**TTAATTA**AATGGGCAGTCGAGTTGGGGAGTTC	32	*Pac*I	
gip1-T1 (CDS)	AGGAATCTGCGGCCAAACATC	21	-	889 bp
gip1-T2 (CDS)	TGGCGCCACATTCAAGACTATCG	23	-	
gip1-T3	CCACCCCGACCCGAAGAGC	19	-	3,711 bp #
gip1-T4	TGGCCACGACATGATATTTTAGCA	24	-	1,918 bp ¤
aurL2-A1	**GAGCTC**CCACCTGATCCGCCCCCATTCTTTG	31	*Sac*I	1,423 bp
aurL2-A2	**CCTAGG**GCCACATCGCACAGCATCAGGTCA	30	*Avr*II	
aurL2-A3	**GGCCGGC**CGATCGTCGTCGTCGGTCAGCATTTA	33	*Fse*I	2,057 bp
aurL2-A4	**CCTGCAG**GACAACCATCCGTCCAGCCGCAACAGA	34	*Sbf*I	
aurL2-T1 (CDS)	AGGTAGACCGTTTTGGCTGATTGT	24	-	589 bp
aurL2-T2 (CDS)	TTGACCCCGGAAAAACCTACC	21	-	
aurL2-T3	CCGTGTGGGAGGTCTTGAGTAAC	23	-	2,740 bp #
aurL2-T4	GGAGGATAGTGAGGGCGTAATAGG	24	-	2,762 bp ¤
hyg1 (Hyg 588L)	GCGCGTCTGCTGCTCCATACAA	22	-	
hyg2 (*aurR1*-D1)	CGTGGCCGGGGGACT	15	-	
Hyg789U	AATAGCTGCGCCGATGGTTTCT	22	-	
FG02325.1 up	CCTAACCATCACGGCCTACAAAA	23	-	379 bp
FG02325.1 low	TTCCTCATAATACCCAACAGTCATC	25	-	
FG02329.1 up	CCGTGTGGGAGGTCTTGAGTAA	22	-	439 bp
FG02329.1 low	ATGGGCAGTCGAGTTGGGGAGTTC	24	-	
lacc2 Exp6 up	ATTTTGGAAGCTTCTGGTTTTTATC	25	-	411 bp
lacc2 Exp6 low	CCCCTTCAAGTGGTCTGGAG	29	-	